

# Objective assessment of limb tissue elasticity: Development of a manual indentation procedure

Yongping Zheng, Arthur F.T. Mak, Bokong Lue, and Arthur F.T. Mak

**Yongping Zheng, PhD; Arthur F.T. Mak, PhD; Bokong Lue, BSc**

*Rehabilitation Engineering Center, The Hong Kong Polytechnic University, Kowloon, Hong Kong*

**Abstract**—An ultrasound indentation system with a pen-size hand-held probe was developed and used to obtain the effective Young's moduli of forearm and lower limb soft tissues in 12 subjects. Since the probe is manually driven, the alignment of the probe and control of the rate of indentation are parameters upon which the results obtained depend. This paper addresses whether manual indentation tests with the probe are sufficiently acceptable and repeatable for objective biomechanical characterization of limb tissues. Forearms of three normal subjects were tested in two states of muscular contraction. Six different indentation rates, ranging from 0.75 mm/s to 7.5 mm/s, were imposed. The load-indentation responses obtained were shown to be well represented by quadratic functions. A linear elastic indentation solution was used to extract the effective Young's modulus. The material parameters extracted were repeatable and rather rate-insensitive for the range of rates used. The effective Young's modulus obtained was found to significantly increase as a result of contraction of the underlying muscles. Indentor misalignment experiments demonstrated that misalignment affects the measurement from which the effective Young's modulus of soft tissues is calculated. This effect, however, was found to decrease as the tissue thickness increased. With the investigation of the above issues, a procedure has been established for the extraction of effective Young's moduli of limb soft tissues from manual cyclic indentation responses. Tests on experimental subjects' lower limbs

further demonstrated that the ultrasonic indenter is a feasible instrument for characterization of the biomechanical properties of limb soft tissues. Paired-t tests showed that the effective Young's moduli of the lower limb soft tissues of three elderly persons with transtibial amputation were significantly smaller than those of six unimpaired young subjects.

**Key words:** *CAD/CAM, indentation test, prosthetics tissue biomechanics, residual limb assessment, soft tissue biomechanics, tissue mechanics, ultrasound instrumentation.*

## INTRODUCTION

Palpation on the skin is widely used clinically to assess the biomechanical characteristics of the residual limb tissue of persons with amputation, due to the lack of an easy-to-use quantitative tool to assess the biomechanical properties of limb tissues. Palpation produces a subjective assessment and, therefore, requires substantial clinical experience. In addition, the qualitative nature of such assessments makes the accumulation of knowledge difficult and teaching/learning imprecise.

During the last decade, computer-aided design and computer-aided manufacturing (CAD/CAM) technologies were introduced to prosthetic socket design (1-9). However, exactly how a socket is designed still depends on the experience of the prosthetist and his or her subjective assessment of the patient's residual limb tissues. The quantitative biomechanical properties of soft tissues have not been

This material is based upon work supported by the Research Grant Council of Hong Kong, Hong Kong SAR, P.R. China.

Address all correspondence to: Prof. Arthur F.T. Mak, Rehabilitation Engineering Center, The Hong Kong Polytechnic University, HungHom, Kowloon, Hong Kong, email: [rcafmak@polyu.edu.hk](mailto:rcafmak@polyu.edu.hk)

included and used in current commercial CAD/CAM socket design systems.

Finite element (FE) analysis has been used by several research groups to study the interface stresses between the surface of the residual limb tissue and the socket (10-34). Biomechanical properties of the residual limb tissues are required inputs for residual limb FE models. Finite element methods, together with information on limb tissue properties, can be integrated into CAD/CAM socket design systems to realize the full potential of CAD/CAM techniques.

Among the various mechanical materials testing methods that have been utilized, indentation testing is probably the most popular technique for determining the *in-vivo* mechanical behavior of skin and limb soft subcutaneous tissues. In 1912, Schade developed an indentation apparatus to study the creep properties of skin and the changes that result from edematous conditions (35). Since then, a number of indentation apparatus have been developed to investigate human soft tissues *in vivo* for various purposes (19,20,23,26-30,36-48). Indentation testing is an effective and relatively straightforward way to assess biomechanical properties of the skin and subcutaneous tissues under compression. The test itself very much resembles the situation of palpation. However, most of the indentation apparatus reported in the literature were developed for research purposes and are not yet ready for routine clinical application. In addition, since the tissue thickness was not monitored, the load-indentation data represented both the geometric effects as well as the material properties of the limb soft tissues.

An ultrasound indentation apparatus was developed by the investigators for the assessment of the mechanical properties of limb soft tissues (49-53). The indentation apparatus consists of a pen-size, hand-held indentation probe (**Figure 1**).

A cylindrical flat-ended ultrasound transducer with a diameter of 9.0 mm and a frequency of 5 MHz is at the tip of the indenter and serves as the indenter probe. The thickness and deformation of the soft tissue layer are determined from the ultrasound echo signal. A compressive 10 N load cell is connected in series with the ultrasound transducer to record the corresponding force response. A schematic of the ultrasound indentation system is shown in **Figure 2**. The accuracy of the deformation and thickness determined by the system was better than 0.02 mm, and the accuracy of the force result was better than

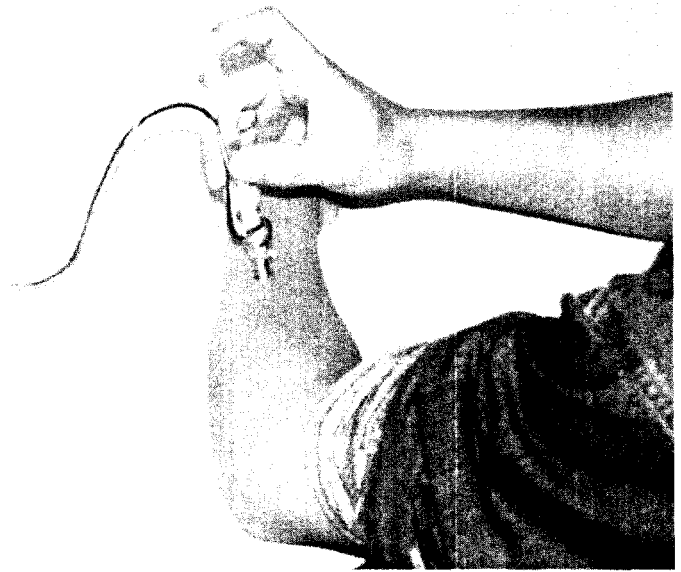


**Figure 1.**

Demonstration of the indentation test using the pen-size hand-held indenter on the forearm of a test subject.

0.003 N (53). The sampling rate was 12.5 data points per second.

Hayes et al. presented a rigorous mathematical solution to the elasticity problem of indentation of a thin, elastic, homogenous layer of material bonded to a rigid half-space (54). The solution yields an expression for calculation of the Young's modulus from the indentation load-deformation data:

$$E = \frac{(1 - \nu^2)}{2\alpha\kappa(\nu, a/h)} \frac{P}{w} \quad [1]$$

where  $P$  is the applied force,  $w$  the indentation depth,  $a$  the radius of the indenter,  $\nu$  Poisson's ratio of the

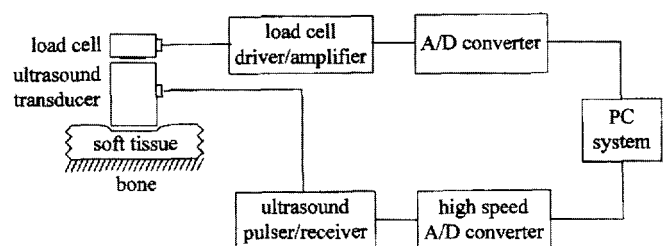


**Figure 2.**

A schematic showing the ultrasound indentation system.

tissue,  $h$  the tissue thickness, and  $k$  a scaling factor. The scaling factor  $k$  provides a theoretical correction for the finite thickness of the elastic layer, and it depends on both the aspect ratio  $a/h$  and Poisson's ratio  $\nu$ . Equation 1 was first developed for the study of articular cartilage, and was later used to extract Young's modulus of limb soft tissues (19,20,24). When the aspect ratio  $a/h$  is small enough (i.e., the tissue thickness is large enough compared with the radius of the indenter), the scaling factor  $k$  tends to be 1. In this case, the load-indentation response is independent to tissue thickness  $h$ . Some investigators calculated Young's modulus of lower limb soft tissues using Equation 1 with this assumption (30). Since the soft tissues are assumed to be homogenous in this solution, the modulus extracted using Equation 1 can be regarded as an effective Young's modulus or effective elastic modulus for the full-thickness bulk tissue. Equation 1 assumes the indenter is perpendicular to the skin surface and to the underlying bony interface. Numerical methods have also been developed to extract from the indentation data parameters governing the biomechanical responses of the limb tissues (19,20,23,24,26,27,47). The ultrasound indentation system allows  $P$ ,  $w$ , and  $h$  to be determined experimentally.

As indentation with the hand-held probe is manually driven, the rate of indentation cannot be controlled precisely. Misalignment of the indenter is also difficult to avoid when the indentation is manual or automated, without *a priori* knowledge of underlying skeletal geometry, orthogonal alignment is not always easy to achieve. The objective of the work reported in this paper is to address whether indentation testing, using the ultrasound hand-held indentation probe, provides a feasible approach for objective biomechanical characterization of limb tissues. In particular, the issues of the indenter misalignment, the rate-sensitivity, and the nonlinearity of the tissue properties were examined.

The validity of the load, deformation, and tissue thickness determined by the ultrasound indenter has been previously verified in a mechanical testing machine (52). To test the feasibility of using the new approach, fresh fish tissues and porcine tissues have been used at the beginning of the study. Results of the misalignment studies are presented here. To assess the adequacy of the ultrasound indenter as a clinically feasible procedure, we investigated the material properties of forearm soft tissues with the underlying

muscles in either relaxed or contracted states. Additionally, the material properties of lower limb soft tissues at bony areas of subjects with and without amputation were investigated. These data are intrinsically important and relevant to the design of prosthetic sockets.

## METHODS

### Experiments on Indenter Misalignment

Using the ultrasound indentation apparatus, *in vivo*, indentation tests were conducted manually by pressing the probe into the skin and soft tissues of the subjects. The apparatus was designed so that indentation testing would be performed without any complicated attachment jig; thus, making it clinically convenient for residual limb assessment. Instead of assuming the displacement of the indenter to be the deformation of the soft tissue layer as used in most of the previous indentation apparatus, the tissue deformation was determined, in this study, from the ultrasound echo reflected from the bone-soft tissue interface. To obtain the largest reflected ultrasound signal, the indenter should be perpendicular to the underlying bone surface. If the probe was not perpendicular to the bone, misalignment would also influence the received ultrasound signal, from which the original tissue thickness and the subsequent tissue deformation are derived.

An *in vitro* experiment on a porcine tissue layer was performed to study the effect of misalignment on the ultrasound reflection signals. The hand-held indentation probe was fixed in line with the load cell of a Hounsfield material-testing machine. A fresh porcine tissue layer with dimensions roughly of 100 x 100 x 25 mm was placed in a container. It was filled with saline solution and was installed on a slanting device, with which the orientation of the bottom of the tissue layer could be adjusted. The indentation was conducted at the center of the layer. Thickness of the entire tissue layer underneath the testing site was 24.5 mm. The probe was first driven by the machine to touch the surface of the tissue layer with a very small preload of 0.02 N. Then the ultrasound echo waves, reflected from the bottom interface of the porcine tissue layer with probe misalignment up to 12.5°, were recorded and compared.

The second experiment concerning misalignment was performed *in vivo* on the left forearm of an unimpaired young male subject. Three sites with

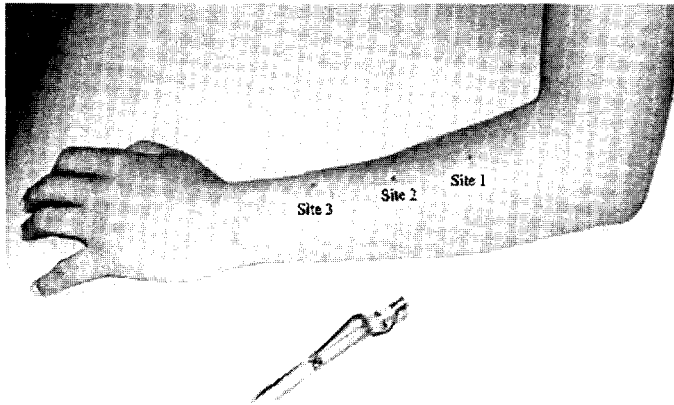


**Figure 3.**  
The three testing sites for the in-vivo experiments of indenter misalignment.

different thickness of soft tissues over the radius were selected as shown in **Figure 3**. The subject sat in front of a table and put his left arm on the surface of the table with the hand and fingers relaxed. Two groups of tests were conducted at each testing site. In the first group of tests, the probe was aligned to maintain a maximal ultrasound echo signal reflected from the bone surface. Five trials were recorded at each site. In the second group of tests, the orientation of the probe was adjusted while still maintaining a small yet acceptable amplitude of ultrasound reflection signal for signal processing. The amplitude in this case was approximately 15 dB less than the maximum amplitude obtained for the maximal signal alignment at the same site, and the orientation of the probe corresponded to a misalignment of approximately  $5^\circ$  along the lateral-medial direction, and approximately  $10^\circ$  along the proximal-distal direction. The degree of misalignment was measured by an electrogoniometer (Model XM110, Biometrics Ltd., Cwmfelinfach, Gwent, UK). A total of 20 trials was performed along different directions at each testing site.

### Experiments on Indentation Rate and Muscular Contraction

Three unimpaired young men, 29, 30, and 32 years old, were involved in this series of tests. The test site was at the soft tissues covering the left radius, about 10 cm distal from the elbow joint. The tissues tested involved skin, fat, and the underlying muscle. **Figure 1** shows the test configuration used.

The subject was instructed to sit in front of a table and put his left arm on the supporting surface. The

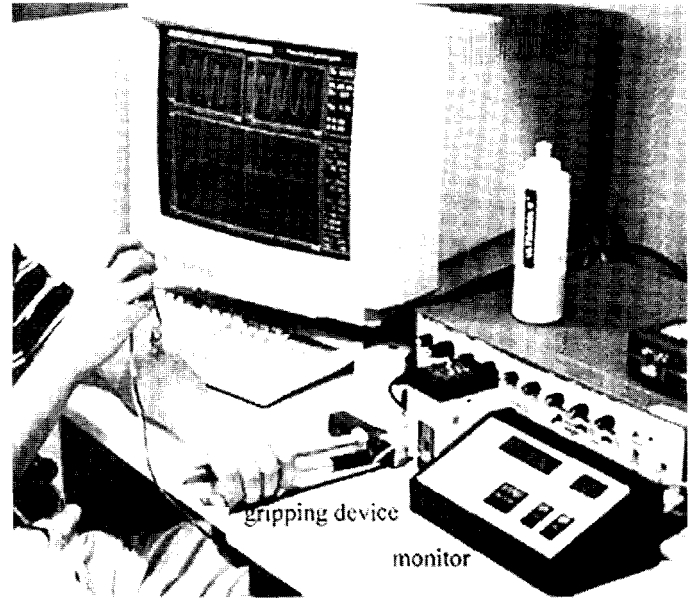


**Figure 4.**  
The experimental setup used to study the effects of muscular contraction on the respective tissue mechanical properties.

angle of the elbow was approximately  $100^\circ$ , the angle between the upper arm and the supporting surface was approximately  $30^\circ$ , and the angle between the upper arm and the shoulder was approximately  $90^\circ$ . The tests were conducted in two states of muscular activation. In the first group of tests, the subject was instructed to relax his wrist and fingers and put his palm and fingers on the supporting surface along the same direction of the forearm. In the second group of trials, the subject was instructed to exert a 5-kg gripping force with his left hand during the test, and then to relax for about 2 minutes. The gripping force was monitored by a device that was developed in our Center for grip training. **Figure 4** shows the experimental setup for this test. Subjects were asked to maintain a stable muscular activation state during the test by monitoring the LED readout of the gripping device.

The indentation was performed with the ultrasound hand-held probe. A couplant gel was used to acoustically couple the ultrasound transducer with the subject's soft tissues. By monitoring the indentation measurement data shown on the screen of the computer, the maximum indentation was controlled and limited to within approximately 30 percent of the initial thickness of the soft tissues. The maximum indentation load was limited to 5 N. Such indentation on the forearm soft tissues with the two

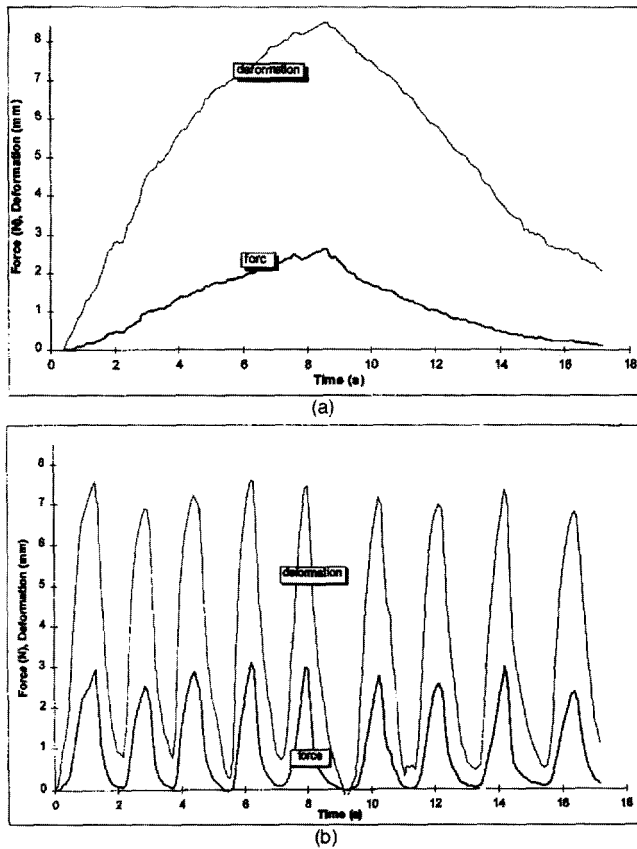


**Figure 5.**

Typical indentation responses recorded on the forearm of subject #1 with the forearm musculature relaxed. Indentation rates of approximately (a) 0.75 mm/s and (b) 7.5 mm/s were used. The original thickness of the soft tissue layer was 19.6 mm.

muscular states could be accepted by the subjects without obvious discomfort. Before each group of tests, three to four trial tests were performed at the test site to maximize and stabilize the ultrasound reflection signal from the surface of the bone; the soft tissues were also preconditioned during this process (55). From the trial tests, the load cell was offset-adjusted so that its reading was zero N when no force was applied. To reduce effects other than indentation rate by averaging, up to six trials were conducted at a similar indentation rate for each test. The rate was estimated by monitoring the force and deformation curves shown on the screen. Six different indentation rates, ranging from 0.75 mm/s to 7.5 mm/s, were imposed at each site for each muscular contraction state. **Figures 5a** and **5b** demonstrate two typical indentation sequences with a rate of approximately 0.75 mm/s and 7.5 mm/s, respectively. These indentation rates were regarded as within the general range that manual indentation could be imposed.

When the indentation rate was lower than 0.75 mm/s, it was difficult to control the loading and unloading sequence smoothly by hand. This may be observed to some degree from the indentation responses shown in **Figure 5a**. On the other hand, when the indentation rate was higher than 7.5 mm/s, the skin surface did not follow the probe during the unloading phases. The repeatability tests were conducted on one subject in a relaxed muscular state using a rate of approximately 4 mm/s. Six tests were measured there and each test comprised up to six trials. Their results were used to verify the repeatability of tests and to investigate how many trials were adequate for a single test.

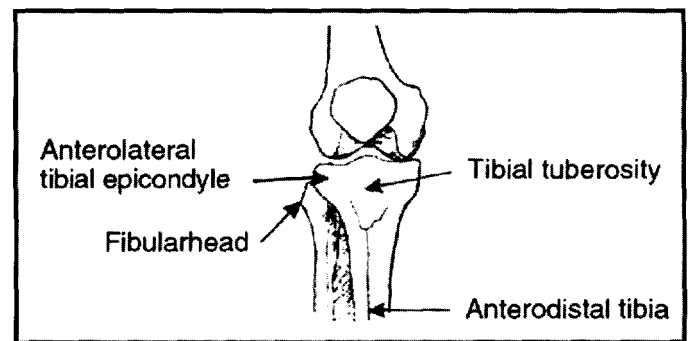


**Figure 6.**

The testing regions used in experiments on lower limb tissues' material properties.

### Experiments on Lower Limbs

Six unimpaired subjects and three subjects with transtibial amputation participated in this series of tests. The mean age of the subjects without amputation was 21.8, and that of subjects with amputation was 63.8. The residual limbs of the test subjects were of cylindrical shape and free of edema. The subjects had worn their prostheses successfully for at least 1 year and were not further categorized by the level of amputation and the period of post-amputation. The sockets the subjects wore were the patella tendon bearing (PTB) type or other PTB variants.

A previous study documented the indentation properties of several pressure-tolerant areas of residual limbs of persons with transtibial amputation (44). However, little attention has been paid to the pressure sensitive or bony-prominent area. **Figure 6** shows the locations on the lower leg at which the indentation tests were performed. In the study, the location of the sites was mainly identified by palpation. The four sites at which the tests were performed were the tibial tubercle, the anterolateral

tibial tubercle, the fibula head, and the anterodistal tibia. Both the amputated side and the contralateral sound side of subjects were tested. In the cases of the subjects without amputation, both the right and left legs were tested.

The location of the anterodistal tibial test site was different in each of the subjects, depending on the length of their residual limb. The anterodistal tibia was defined as the most anterior and distal bone prominence of the tibia. After selecting the anterodistal site, the distance from the center of the patella to the anterodistal tibia was recorded. The same distance at the sound side was used to locate the corresponding site. For the unimpaired subjects, the anterodistal tibia was defined at about 16.5 cm from the center of the patella. The dimension of 16.5 cm was the mean distance for the subjects with amputation.

During the test, the subjects sat on an adjustable height chair. The condition of their (residual) limb soft tissue was examined and recorded. The dimensions of their (residual) limbs were measured including length and circumference at different levels. By adjusting the height of the chair, the angle between the lower leg and the thigh was set at 90°, with the lower leg placed perpendicular to the floor. A goniometer was used to monitor the knee angle. Following a similar testing procedure described previously for the forearm tests, two trials were performed at each site, noting that the extracted effective Young's modulus was quite repeatable, based on the results of the preliminary studies. The maximum force applied was kept below 4 N to avoid

discomfort to the subjects. Finite element analysis showed that the pressures applied to these areas of the residual limb-socket interface were in a similar range (32).

### Preliminary Observations

Nonlinear behavior and hysteresis were observed in the load-indentation curves recorded at the various sites and indentation rates tested. **Figure 7** shows the experimental data points measured for a typical load-indentation response test of forearm soft tissues.

The data points of the loading phase were labeled with square marks, and those of the unloading phase were labeled with cross marks. It was found that the following quadratic function could well represent the load-indentation relationship with the coefficient of determination  $R^2$  generally greater than 0.9:

$$P = C_0 + C_1 w + C_2 w^2 \quad [2]$$

where  $P$  is the indentation load,  $w$  the indentation depth,  $C_0$ ,  $C_1$ , and  $C_2$  the coefficients that represent the indentation behavior of the tissue. The data points of the loading and unloading phase were both involved in this curve fitting process. The derived coefficients represented not only the material properties of the soft tissue, but also other geometric factors, such as the indenter diameter and the tissue

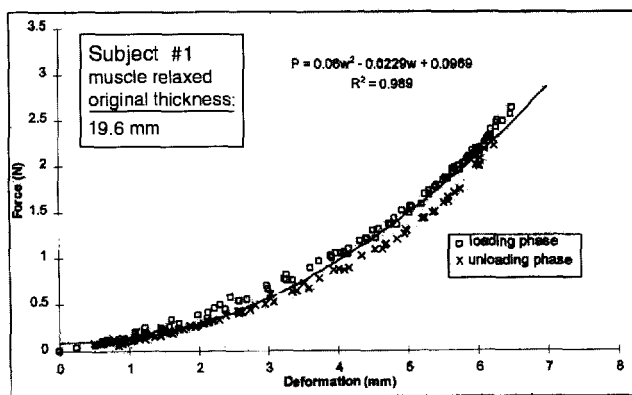


**Figure 7.** Typical load-indentation measurements obtained from a forearm test subject, and the corresponding quadratic regression curve fit to the data.

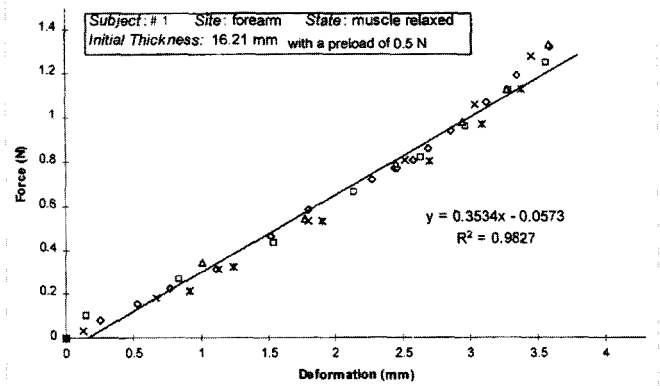


**Figure 8.** The selected data points used for the estimation of the effective Young's modulus of tissue. Different symbols represent the data points of different cycles. The data in the loading phases with the indentation load greater than 0.5 N and less than 75 percent of the maximum value were selected. The plotted data were rescaled from the raw data assuming the 0.5 N preload point to be the reference state.

thickness, viscoelasticity, and stiffness.

### Data Reduction Methods

The effective Young's modulus was calculated using Equation 1, and the Poisson's ratio  $K$  was assumed to be 0.45. The diameter of the indenter (i.e., the ultrasound transducer) was 9.0 mm in this study. With these constants, Equation 1 can be written in the form:

$$E = \frac{1}{K(h)} \cdot \frac{P}{w} \quad [3]$$

where  $K(h)$ , with a dimension of length, is a factor only depending on the thickness  $h$  of the soft tissue if a constant Poisson's ratio  $n$  is assumed. Using the value of  $k(a/h, n)$  determined by Hayes et al. (54), the relationship between  $K(h)$  and thickness  $h$  can be derived.  $K(h)$  can be interpolated for an arbitrary value of  $h$ .

A typical indentation response is shown in **Figure 7**. In this specific test, five loading-unloading cycles were manually performed within a testing period of about 17 seconds. The load-indentation curve shows the typical nonlinear and viscoelastic characteristics of the soft tissues. During the indentation test with the probe manually driven, the indentation rate could only be approximately controlled. The experimental data points in the loading phases with the indentation load greater than 0.5 N and less than 75 percent of the maximum value of 5.0 N were selected for the following data analysis to estimate the effective Young's modulus. It was noted that the indentation

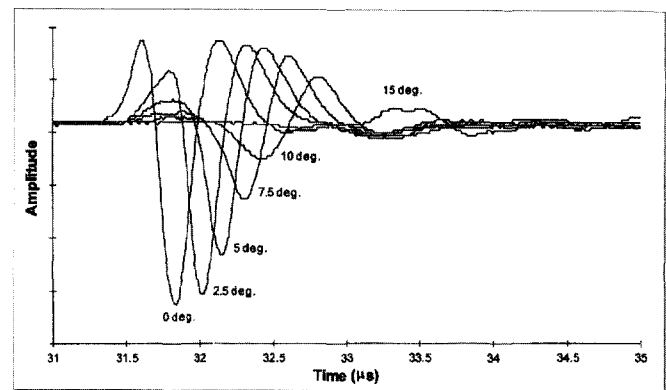


**Figure 9.**

Recorded ultrasound echo signals, which were reflected from the bottom interface of a layer of fresh porcine tissue, showing the various degrees of indenter misalignment used.

rate was relatively more difficult to control outside this range. The selected data points within such limits were plotted in **Figure 8** with different symbols representing the data points of different cycles. With the limitations on the selection of data points, the nonlinear properties of the load-indentation response in **Figure 7** have been reduced. The data point with the first 0.5 N load reading was defined as the initial state. The soft tissue thickness at this state was defined as the initial thickness. A linear regression was used to fit the experimental data. The slope of the curve was the mean ratio of load to indentation (i.e.,  $P/w$ ), which is related to the biomechanical properties of the soft tissue according to Equation 3. The small offset was a result of the linear regression of the mildly nonlinear force-deformation data. For the forearm test shown in **Figures 7** and **8**, the initial

**Table 1.**

Effective Young's moduli and thicknesses of the forearm soft tissues at the three testing sites with two different alignment states of the probe.

	Site 1		Site 2		Site 3	
	Mean	SD	Mean	SD	Mean	SD
<b>Modulus (kPa)</b>						
Test A	20.39	1.81	37.41	1.81	34.74	1.94
Test B	19.35	0.76	33.96	1.98	21.33	0.91
<b>Thickness (mm)</b>						
Test A	17.50	0.13	15.14	0.21	8.80	0.12
Test B	17.63	0.18	15.61	0.20	8.94	0.13

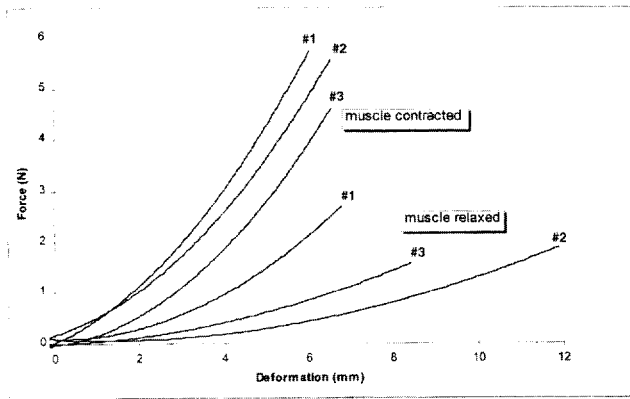


**Figure 10.** Comparison of the regression curves of the load-indentation data among subjects. The indentation data were taken on the forearm under two different muscular contractile states. Subjects 1, 2, and 3 were the three subjects in this series of tests.

thickness  $h$  was determined as 16.2 mm with a preload of 0.5 N,  $K(h)$  was calculated to be 15.6 (mm), and the average ratio of the applied load to the indentation depth  $P/w$  obtained from the linear regression was 0.35 N/mm. The effective Young's modulus was then calculated to be 22.6 kPa using Equation 3.

**RESULTS**

**Indenter Misalignment**

**Table 1** presents the effective Young's modulus and thickness of forearm soft tissues at the three testing sites shown in **Figure 3** calculated using Equation 3 and the measurements acquired with two different alignments of the probe. The measured tissue thickness varied slightly between the two different alignment cases at all three sites. However, the resulting effective Young's modulus computed, decreased at all three test sites as the probe misalignment increased. This misalignment effect was the greatest at the site with the thinnest soft tissue. A: Aligning the probe with the amplitude of the ultrasound reflection signals being maximal. Test B: Aligning the probe with a minimal acceptable ultrasound reflection signal, corresponding to a misalignment of approximately  $\pm 10^\circ$  to the normal to the radial shaft along the proximal-distal direction, and of approximately  $\pm 5^\circ$  to the normal to the radial shaft along the medial-lateral direction.

**Figure 9** shows the ultrasound echo signals recorded after reflection from the bottom interface of the fresh porcine tissue specimen. A slight time shift

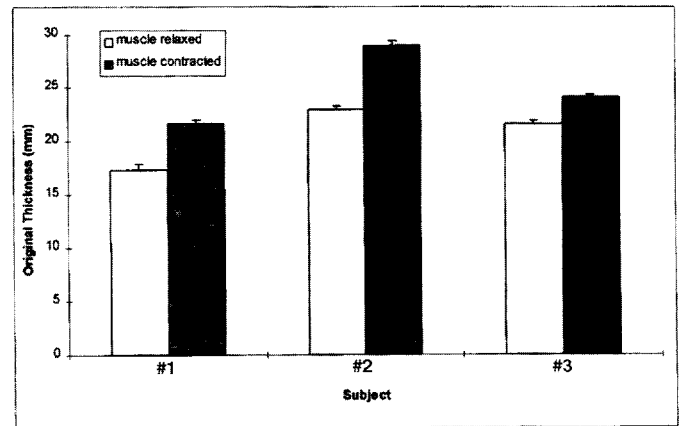


**Figure 11.** Original thickness of soft tissues at the indentation sites of the three subjects under two different muscular contraction states.

of the ultrasound signal of up to approximately 2 percent was observed as the probe misalignment increased from  $0^\circ$  to  $10^\circ$ . This time shift would cause a small error in the measured thickness, but would not affect the derived indentation. The amplitude of the echo signal was significantly reduced as the degree of misalignment increased from  $0^\circ$  to  $15^\circ$ . These characteristics can be used to empirically maintain a reference alignment of the probe during the manually activated indentation. These phenomena can be ascribed to the behavior of ultrasonic signal

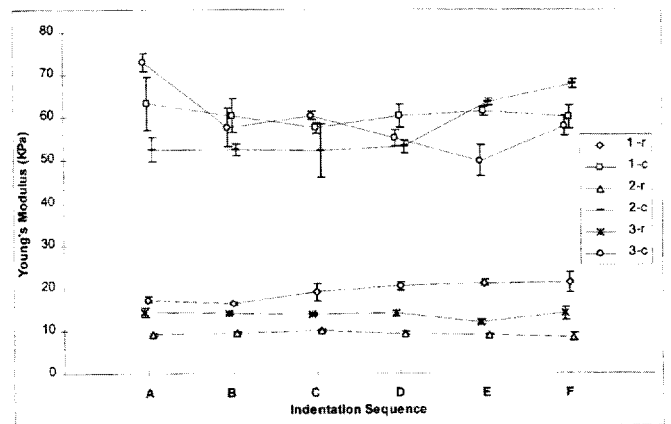


**Figure 12.** The relationship between effective Young's modulus,  $E$ , of forearm soft tissue and indentation rate. The error bar represents the standard deviation of the four trials. "A" to "F" represent the six different indentation rates. "4-r" indicates the tests of subject #4 with the forearm and the hand relaxed, and "4-c" indicates the tests with the hand exerting a 5-kg gripping force.



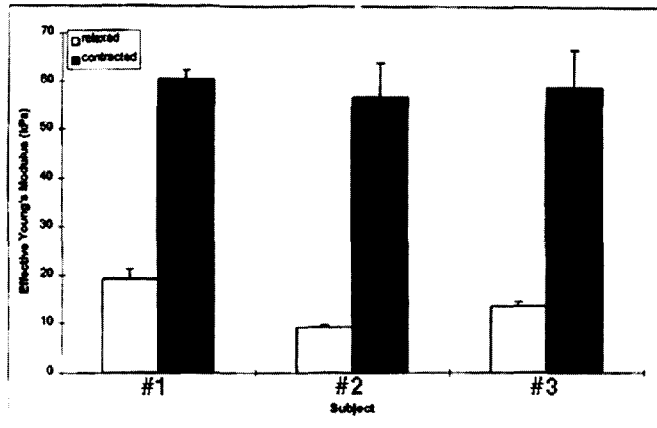


**Figure 13.**

Variation of the effective Young's modulus,  $E$ , of the forearm soft tissue as a function of the underlying muscular contractile state. The error bar represents the standard deviation of the results of the six groups of tests using different indentation rates.

propagation. When the surface of the ultrasound transducer is not parallel to the reflecting interface, the signal is not entirely spectrally reflected, and thus, is not completely received by the transducer. An additional propagation path would be induced, and rough osseous reflecting surfaces cause wavelet model cancellation.

### Indentation Rate and Muscular Contraction

**Figure 10** shows the comparison between the regression curves of the forearm indentation responses recorded from the three subjects with the underlying muscles both relaxed and contracted. Differences among individuals can be noted from the curves. Significant changes in the measured indentation responses were observed for the subjects as a function of the underlying state of their muscular activation.

**Figure 11** shows the thicknesses of the soft tissue layers, measured at the forearm test sites, of the three subjects for two different states of muscular contraction. The mean tissue thickness and respective standard deviations were calculated for each subject from a total of 36 trials each. The soft tissue thicknesses were found to increase by 25, 26, and 11 percent for subjects #1, #2, and #3, respectively, as they contracted their underlying muscles.

In a study of measurement, a total of six tests were conducted, in which six trials were performed for each test. The percentage standard deviations in the calculated values of the effective Young's modulus,  $E$ , among the six tests were all less than 3

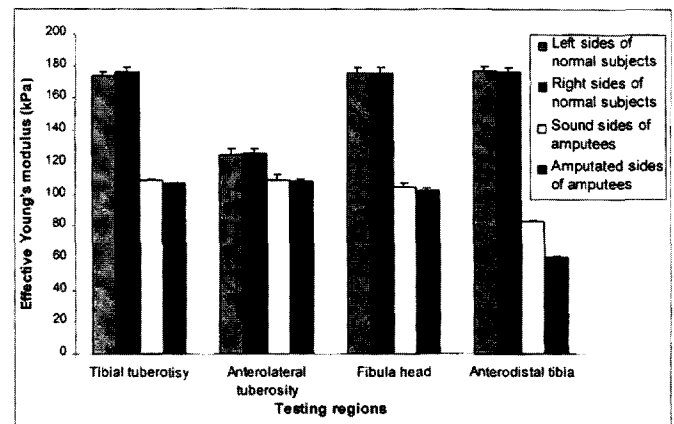


**Figure 14.**

The comparison of the effective Young's moduli obtained for the subjects with and without amputation.

percent. The percentage standard deviations of the original measured tissue thickness were found to be less than 2 percent. The small variations obtained suggested that the extracted material parameters were repeatable.

The mean percentage standard deviation of the effective Young's modulus,  $E$ , obtained from the tests of the three subjects under two muscular contraction states using six different indentation rates was 8.4 percent. The maximum value (13.0 percent) and the minimum value (3.2 percent) were observed from subject #3 and subject #1 with muscle contracted, respectively. The effect of variations in indentation rate on the values extracted for the effective Young's modulus of the subjects, therefore, was not dramatic for the range of indentation rates tested, that is, from 0.75 mm/s (rate A) to 7.5 mm/s (rate F), as shown in **Figure 12**. The effective Young's modulus of limb soft tissues thus appears to be reasonably rate-insensitive within this range.

**Figure 13** shows the effective Young's moduli of the forearm soft tissues significantly increased from  $14.0 \pm 5.0$  kPa to  $58.8 \pm 1.7$  kPa as a result of contraction of the underlying muscles. These results were calculated from the mean values from the tests of the three subjects with their relevant muscles relaxed and contracted respectively. This shows that the subjects' soft forearm tissues became significantly stiffer when the underlying muscles were contracted.

### Lower Limb Tests

**Figure 14** represents the variation of the effective Young's modulus of the lower limb soft tissues

measured at different sites on both limbs for the test groups with and without amputation. Generally, the effective Young's moduli of the sound limbs of the subjects with amputation were greater than those obtained for their residual limbs. However, the difference was rather small except at the anterodistal tibia. For the tibial tuberosity, anterolateral epicondyle, and fibular head, paired-t comparisons between the measurements on the residual limbs and on the sound limbs did not demonstrate significant difference. For the site over the anterodistal tibia, however, paired-t tests showed a significant difference between the effective Young's moduli of the residual limbs of the subjects with amputation and that of their contralateral sound limbs. It may also be seen in **Figure 14** that the effective Young's moduli of the young unimpaired subjects were higher than those of the elderly subjects with amputation. A similar result was reported earlier by other investigators using an electromechanical indentation system (44).

## DISCUSSION

### Indentation Response

A newly developed ultrasound apparatus was used to obtain the indentation responses of forearm soft tissues. Three unimpaired forearms were tested with two muscular contraction states. Quadratic functions were found to be adequate to represent the load-indentation responses. Silver-Thorn used a third order polynomial to fit the load-indentation response recorded on the below-knee residual limbs within the confinement of a prosthetic socket (23). It should be noted that the indentation responses of the soft tissue not only depended on the mechanical behavior of the soft tissues, but also on the soft tissue thickness, the initial state of the soft tissue, the boundary interface conditions, and the indenter geometry.

### Soft Tissue Thickness

Tissue thickness is an important parameter in determination of the material properties of the tissue from indentation response measurements, especially when the indenter diameter and the tissue thickness are comparable (54). In the literature, there have been reports on the use of CATSCAN, X-rays, and MRIs to estimate tissue thicknesses at indentation sites on test subjects' (residual) limbs (19,26,30). Ultrasound has also been used to measure the thickness of soft tissues (42,44). In the current study, soft tissue

thickness was estimated continuously during indentation using ultrasonic pulse/echo analysis technique. Thickness measurement is an inherent result of the present indentation technique and can be readily incorporated into data reduction and analysis procedures. Significant changes of the soft tissue thickness were found due to changes of underlying musculature activation states. The thickness of forearm bulk soft tissues was found to increase by up to 26 percent as test subjects contracted their underlying muscles, exerting a 5 kg palmar prehension gripping force.

### Repeatability

The extracted material parameters obtained in this study were repeatable at a given site for a given individual with a given state of muscular activation. The percentage standard deviation of the measured tissue thickness was less than 2 percent. The effective Young's modulus extracted using the linear elastic model showed a percentage standard deviation of less than 3 percent.

### Effects of Indentation Rate

It is known that the mechanical behavior of limb soft tissues generally shows time-dependent phenomena (e.g., hysteresis). The influences of indentation rate on tissue mechanical response were reported by Reynolds and by Torres-Moreno (19,30). The loading rates studied by Reynolds were 0.3, 0.8, and 1.3 mm/s. Those investigated by Torres-Moreno were 9.9, 14.2, and 19.8 mm/s. Their indentors, however, were attached to the prosthetic socket, and were driven by mechanical actuators into test subjects' soft tissue through ports in the sockets. In the current study, the indentation probe was manually driven, and the mean indentation rates used in the current study ranged from 0.75 to 7.5 mm/s. This range of indentation rates was approximately in the middle between that used by Reynolds and that used by Torres-Moreno. This was found to be the manageable range of rates imposable by hand. The Young's moduli determined from the ultrasonic indentation probe measurements were found to be relatively insensitive to the indentation rate, with a *percentage standard deviation* of less than 10 percent for the range of indentation rates imposed. Torres-Moreno demonstrated that the effect of indentation rate was different at different testing sites, and also with a different load level (30). Reynolds reported that the

effect of indentation rate on the indentation response was more serious when greater loads were applied (19). In the experiments of Torres-Moreno and Reynolds, the average maximal pressure applied to obtain a certain amount of deformation was much greater (about 5 times) than that used in the current study because soft tissues were confined by the socket in their studies. This might also be one of the reasons why hysteresis observed in Torres-Moreno's results was generally more serious than that observed in the current study. In the confined tests, the skin would be drawn sideways along the socket wall by the indentation, and additional inelasticity might be induced. The lower load levels used in concert with a 0.5 N preload may have reduced the tissue measurement sensitivities to indentation rate observed in the current study to some degree. Further studies on rate sensitivity under a broader range of conditions, such as higher loading levels, tissue socket confinement, and so forth, warrant further investigation using the current ultrasonic measurement technique.

#### **Effect of Muscle Contraction**

Tissue mechanical response measurements and the associated material parameters derived therefrom varied significantly with changes in the contractile state of the underlying musculature. The effective Young's modulus of proximal forearm tissue significantly increased from  $14.0 \pm 5.0$  kPa to  $58.8 \pm 1.7$  kPa as a result of contraction of the underlying muscles. The two states can be easily differentiated by the obtained effective Young's moduli.

#### **Effect of Poisson's Ratio Assumed**

In the current study, a Poisson's ratio of 0.45 was assumed for the soft tissue in calculation of Young's modulus for the tissue tested. If the Poisson's ratio was assumed to be 0.3 or 0.5, instead of 0.45, the extracted effective Young's modulus increased by 19 percent, or decreased by 8.6 percent, respectively, for a tissue thickness of 20 mm. This effect becomes more serious when the tissue thickness decreased (53). In most indentation studies on skin and subcutaneous tissues, investigators have assigned a Poisson's ratio within the range of from 0.45 to 0.5 to simulate the "nearly incompressible" behavior of the soft tissues as a whole (19,23,25,30,39,44,47). The Poisson's ratio of the limb tissues *in vivo* merits further investigation.

#### **Effects of Indentor Misalignment**

The misalignment of the indenter is an important issue for indentation testing. Previous *in-vitro* experiments on a fresh fish tissue layer demonstrated that the indentation responses can be influenced by the misalignment of the indenter, especially at sites with soft tissue thickness comparable to the diameter of the indenter (53). It was observed with up to  $12.5^\circ$  misalignment of the indenter, the effect on the indentation response decreased as the tissue thickness increased, and became almost negligible when the thickness was greater than double that of the indenter diameter. Similar results were obtained from the *in-vivo* experiment on test subjects' forearms in this study. The effective Young's modulus obtained with approximately  $5-10^\circ$  of misalignment was smaller than that obtained with the maximum strength signal alignment. This effect was the most pronounced when the tissue thickness was comparable to the indenter diameter. Fortunately, alignment of the ultrasonic indentation probe for maximum echo signal strength is readily accomplished. The amplitude of the ultrasonic echo signal decreases as the marked degree of misalignment of the indenter is increased, while the time shift of the ultrasonic signal increased only slightly. The sensitivity of the ultrasonic amplitude signal to misalignment can be used as constructively as feedback for initial determination and subsequent maintenance of correct indenter alignment during *in-vivo* indentation testing.

#### **Results of Lower Limb Soft Tissues**

The experiments on the lower limbs of subjects with and without transtibial amputation demonstrated that the ultrasound indentation probe was feasible for the biomechanical assessment of limb soft tissues *in vivo*. No significant difference was established by paired-t comparisons between the measurements at the sites of the right limbs and those of left limbs of unimpaired subjects. However, results showed that the effective Young's moduli of lower limb soft tissues of the six unimpaired young subjects were significantly greater at the four testing sites than those of the three elderly subjects with amputation. Similar results have been obtained previously by using a mechanically driven indenter (44). The variation of the effective Young's modulus was due mainly to age rather than to amputation. This statement was supported by the finding that the difference between the effective Young's moduli of the sound limb tissues

and those of the amputated sides of the same subjects were quite small. The age dependence of the biomechanical properties of biological soft tissues is previously documented (55). Paired-t tests demonstrated that the effective Young's moduli of the residual limb tissues were significantly smaller than those of their sound sides at only the site of anterodistal tibia. Significant differences were not observed at other three sites. The soft tissues at the anterodistal tibia of the residual limb apparently have degraded at a higher rate than the corresponding site on the sound side. The previous study demonstrated that the Young's modulus of the residual limb tissues in three load-tolerant areas became slightly greater when it was tested at approximately 6 months after the subject began wearing a prosthesis compared with that measured approximately 3 weeks post-amputation (44). However, It is not clear from these two studies whether the changes in the biomechanical properties were due to the biomechanical interactions of the residual limb with the prosthesis or simply due to a natural course of further tissue reconfiguration post-amputation regardless of whether or not the residual limb was loaded. Further investigation of long-term monitoring of the biomechanical properties of residual limbs would be necessary to answer this question. An easy-to-use approach like the one introduced in this paper may facilitate this kind of research.

#### **Limitations and Extensions of the Theoretical Model**

The data reduction method used in this paper is based on Hayes' solution of the indentation problem (54), which assumes that an infinite plane of homogenous isotropic tested material bonded at the bottom to an infinite rigid planar surface, is orthogonally indented at the material upper surface by a frictionless, cylindrical indenter. In reality, in this application, since the reflecting bone surface below the soft tissue is not flat, nor is it large enough to satisfy Hayes' assumed boundary condition, the determined soft tissue thickness can only be treated as an effective thickness. Therefore, the effect of the shape and size of the underlying osseous reflecting surface on the tissue material properties extracted, warrants further investigation, both numerically and experimentally. Friction between the indenter surface and the skin surface can be neglected, since a couplant gel was used to couple the ultrasound signal and the soft tissues.

Infinitesimal deformation is assumed in the mathematical solution proposed by Hayes et al. (54). This assumption was also not satisfied in the indentation tests performed in this study on subjects' skin and subcutaneous tissues. If the indenter diameter and the soft tissue thickness were comparable, the effects of the large deformation should be taken into account when using Hayes' solution. To reduce the large-deformation effect, an indenter with a small diameter can be used. However, the material properties measured in this case may represent the mechanical behavior of the superficial layer of limb soft tissues rather than that of the entire layer. A finite element analysis for a large-deformation indentation problem has been presented (56). It showed that the scaling factor  $k$  in Equation 1 increased as indentation depth increased. For a tissue layer with 20 mm in thickness and an indenter with 9 mm in diameter,  $k$  increased by 5.5 percent from 1.28 to 1.35 when the indentation depth changed from 0.1 percent to 10 percent of tissue thickness. Simply using Hayes' result to calculate Young's modulus for a large indentation depth may produce an error in the result, especially for a large aspect ratio ( $a/h$ ). The results of this numerical study can be used to correct the error caused by a large-deformation problem when extracting the effective Young's modulus from indentation responses.

The mechanical properties of limb soft tissues are generally nonlinear and viscoelastic. This could be observed to some degree in the load-indentation response presented in **Figure 7**. To obtain the effective Young's modulus, the nonlinearity and viscoelasticity were reduced in the data analysis used in this study by excluding the data points near the peak and valley of the indentation cycles and by the linear regression of the data series. Such a simplified material parameter may be particularly useful for comparative studies. For more precise descriptions of biomechanical properties of soft tissues, a quasilinear viscoelastic theory has been used to study the nonlinear and time-dependent behavior of the limb soft tissues (52,53,55). Linear and nonlinear modulus and time constant of soft tissues were extracted from the cyclic load-indentation response by a curve-fitting procedure.

## CONCLUSION

In this paper, the feasibility of using a hand-held indentation probe for the objective assessment of limb soft tissue elasticity has been investigated. Issues relevant to the extraction of the effective Young's modulus were addressed, including test repeatability, indenter misalignment, indentation rate sensitivity, assumption of Poisson's ratio, and the issue of large deformation. Results showed that the extracted Young's moduli of limb soft tissues under similar conditions were well repeatable. The effects of misalignment increased as tissue thickness decreased, especially when the thickness was smaller than the indenter diameter. Sensitivity of the amplitude of ultrasound signal to the misalignment could be used as an indication of correct indenter alignment. The Young's moduli determined using the current data reduction approach were relatively insensitive to the indentation rate with a percentage standard deviation of less than 10 percent for the range of rates appropriate for manual indentation. The assumption of a constant Poisson's ratio of soft tissues at various sites, states of muscular activities and pathological conditions, and for different subjects might cause an uncertainty to the extracted Young's modulus. The error in the use of the Hayes's indentation model due to large deformation can be corrected by the results of the finite element analysis. However, other issues, such as curvatures of the limb surface and underlying bone should be further investigated to examine their effects on the extracted Young's modulus.

With the consideration of the above issues, a procedure has been established to extract the effective Young's modulus from manual cyclic indentation responses. The experiments on forearms with underlying muscle relaxed and contracted and the tests on the lower limbs of subjects with and without amputation demonstrated that the new approach was feasible for the measurement of effective Young's modulus of limb soft tissues. We expect that such a relatively simple approach can be used in the field of prosthetics to objectively assess the mechanical properties of residual limb soft tissues for socket design. The material properties obtained by this approach can be used as an objective reference for prosthetists, as an input to the CAD/CAM socket design systems, or for the finite element modeling of socket-residual limb interface.

## REFERENCES

1. Boone DA, Harlan J. Considerations for computer interface design for prosthetics and orthotics: a user's perspective. Proceedings of the 7th World Congress of ISPO, Chicago; 1992. p. 157.
2. Boone DA, Harlan JS, Burgess EM. Automated fabrication of mobility aids: review of the AFMA process and VA/Seattle ShapeMaker software design. *J Rehabil Res Dev* 1994; 31(1):42-9.
3. Dean D, Saunders CG. A software package for design and manufacture of prosthetic sockets for transtibial amputees. *IEEE Trans Biomed Eng* 1985;32(4):257-62.
4. Ellepola W, Sheredos SJ. Report on the evaluation of the VA/Seattle below-knee prosthesis. *J Rehabil Res Dev* 1993;30(2):260-6.
5. Engsborg JR, Clynch GS, Lee AG, Allan JS, Harder JA. A CAD/CAM method for custom below-knee sockets. *Prosthet Orthot Int* 1992;16:183-8.
6. Houston VL, Burgess EM, Childress DS, et al. Automated fabrication of mobility aids (AFMA): below-knee CAD/CAM testing and evaluation program results. *J Rehabil Res Dev* 1992;29(4):78-124.
7. Lilja M, Öberg T. Volumetric determinations with CAD/CAM in prosthetics and orthotics: errors of measurement. *J Rehabil Res Dev* 1995;32(2):141-8.
8. Saunders CG, Foort J, Bannon M, Dean D, Panych L. Computer-aided design of prosthetic sockets for below-knee amputees. *Prosthet Orthot Int* 1985;9:17-22.
9. Torres-Moreno R, Morrison JB, Cooper D, Saunders CG, Foort J. A computer-aided socket design procedure for above-knee prostheses. *J Rehabil Res Dev* 1992;29(3):35-44.
10. Brennan JM, Childress DS. Finite element and experimental investigation of above-knee amputee limb/prosthesis systems: a comparative study. *Advances Bioeng ASME* 1991;BED-20:547-50.
11. Huang DT, Mak AFT. The effects of sliding between muscle groups on the stress distribution within below-knee stumps. Proceedings of the 8th International Conference on Biomedical Engineering, Singapore; 1994. p. 348-50.
12. Krouskop TA, Muilenberg AL, Dougherty DR, Wittingham DJ. Computer-aided design of a prosthetic socket for an above-knee amputee. *J Rehabil Res Dev* 1987;24(2):31-8.
13. Lee VSP, Solomonidis SE, Paul JP. Mechanical behaviour of amputee stump/socket using finite element analysis. Proceedings of the International Society of Biomechanics XIV Congress, Paris; 1993. p. 774-5.
14. Lee VSP, Solomonidis SE, Spence WD, Paul JP. A study of the biomechanics of the residual limb/prosthesis interface in trans-femoral amputees. Abstracts of the 8th World Congress of ISPO, Melbourne, Australia; 1995. p. 79.
15. Mak AFT, Yu YM, Hong ML, Chan C. Finite element models for analyses of stresses within above-knee

- stumps. Proceedings of the 7th World Congress of ISPO, Chicago; 1992. p. 147.
16. Mak AFT, Huang DT. Stresses within the above-knee stump tissues due to relative motions between the femur and the prosthetic socket. Proceedings of the 2nd World Congress of Biomechanics, Amsterdam; 1994.
  17. Quesada PM, Skinner HB. Analysis of a below-knee patellar tendon-bearing prosthesis: a finite element study. *J Rehabil Res Dev* 1991;28(3):1-12.
  18. Quesada PM, Skinner HB. Finite element analysis of the effects of prosthesis model alterations on socket/stump interface stresses. Proceedings of the 7th World Congress of ISPO, 1992. p. 275.
  19. Reynolds D. Shape design and interface load analysis for below-knee prosthetic sockets (dissertation). University of London; 1988.
  20. Reynolds D, Lord M. Interface load analysis for computer-aided design of below-knee prosthetic sockets. *Med Biol Eng Comput* 1992;1:89-96.
  21. Sanders JE. Ambulation with a prosthetic limb: mechanical stress in amputated limb tissues (dissertation). University of Washington; 1991.
  22. Sanders JE, Daly CH. Normal and shear stresses on a residual limb in a prosthetic socket during ambulation: comparison of finite element results with experimental measurements. *J Rehabil Res Dev* 1993;30(2):191-204.
  23. Silver-Thorn MB. Prediction and experimental verification of residual limb/prosthetic socket interface pressures for below-knee amputees (dissertation). Northwestern University, Illinois; 1991.
  24. Silver-Thorn MB, Childress DS. Use of a generic, geometric finite element model of the below-knee residual limb and prosthetic socket to predict interface pressures. Proceedings of the 7th World Congress of ISPO, Chicago; 1992. p. 272.
  25. Silver-Thorn MB, Childress DS. Parametric analysis using the finite element method to investigate prosthetic interface stresses for person with trans-tibial amputation. *J Rehabil Res Dev* 1996; 33(3):227-38.
  26. Steege JW, Schnur DS, van Vorhis RL, Rovick J. Finite element analysis as a method of pressure prediction in the below-knee socket. Proceedings of the 10th Annual RESNA Conference, San Jose; 1987. p. 814-6.
  27. Steege JW, Schnur DS, Childress DS. Prediction of pressure at the below-knee socket interface by finite element analysis. Symposium on the Biomechanics of Normal and Pathological Gait, Boston, AMSE, WAM; 1987. p. 39-43.
  28. Steege JW, Childress DS. Finite element modeling of the below-knee socket and limb: phase II. Modeling and Control Issues in Biomechanical System Symposium, ASME WAM; 1988. p. 121-9.
  29. Steege JW, Silver-Thorn MD, Childress DS. Design of prosthetic sockets using finite element analysis. Proceedings of the 7th World Congress of ISPO, Chicago; 1992. p. 273.
  30. Torres-Moreno R. Biomechanical analysis of the interaction between the above-knee residual limb and the prosthetic socket, (dissertation). University of Strathclyde, Glasgow, UK; 1991.
  31. Zachariah SG, Sanders JE. Interface mechanics in lower-limb external prosthetics: a review of finite element models. *IEEE Trans Rehabil Eng* 1996;4(4):288-302.
  32. Zhang M. Biomechanics of the residual limb and prosthetic socket interface in below-knee amputees (dissertation). University of London; 1995.
  33. Zhang M, Lord M, Turner-Smith AR, Roberts VC. Development of a non-linear finite element modelling of the below-knee prosthetic socket interface. *Med Eng Phys* 1995;17(8):559-66.
  34. Zhang M, Mak AFT. A finite element analysis of the load transfer between an above-knee residual limb and its prosthetic socket—roles of interface friction and distal-end boundary conditions. *IEEE Trans Rehabil Eng* 1996;4(4):337-46.
  35. Schade H. Untersuchungen zur organfunktion des bindegewebes. *Ztschr Exper Path Therapis* 1912;11:369-99.
  36. Bader DL, Bowker P. Mechanical characteristics of skin and underlying tissues in vivo. *Biomaterials* 1983;4:305-8.
  37. Dikstein S, Hartzstark A. In vivo measurement of some elastic properties of human skin. In: Marks R, Payne PA, editors. *Bioengineering and skin*. Lancaster: MTP Press; 1981. p. 45-53.
  38. Ferguson-Pell M, Hagisawa S, Masiello RD. A skin indentation system using a pneumatic bellows. *J Rehabil Res Dev* 1994;31(1):15-9.
  39. Horikawa M, Ebihara S, Sakai F, Akiyama M. Non-invasive measurement method for hardness in muscular tissues. *Med Biol Eng Comput* 1993;31:623-7.
  40. Kirk E, Kvorning SA. Quantitative measurements of the elastic properties of the skin and subcutaneous tissue in young and old individuals. *J Gerontol* 1949;4:273-84.
  41. Kirk E, Chicffi M. Variations with age in elasticity of skin and subcutaneous tissue in human individuals. *J Gerontol* 1962;17:373-80.
  42. Kydd WL, Daly CH, Nansen D. Variation in the response to mechanical stress of human soft tissues as related to age. *J Prosthet Dent* 1974;32(5):493-500.
  43. Lewis HE, Mayer J, Pandiscio AA. Recording skinfold calipers for the determination of subcutaneous edema. *J Lab Clin Med* 1965;66(1):154-60.
  44. Mak AFT, Liu GHW, Lee SY. Biomechanical assessment of below-knee residual limb tissue. *J Rehabil Res Dev* 1994;31(3):188-98.
  45. Torres-Moreno R, Solomonidis SE, Jones D. Three-dimensional finite element analysis of the above-knee residual limb. Proceedings of the 7th World Congress of ISPO, Chicago; 1992. p. 274.
  46. Vannah WM, Childress DS. An investigation of the three-dimensional mechanical response of bulk muscular tissue: experimental methods and results. In: Spilker RL, Simon BR, editors. *Computational methods in bioengineering*; 1988. p. 493-503.
  47. Vannah WM, Childress DS. Indentor tests and finite element modeling of bulk muscular tissue in vivo. *J Rehabil Res Dev* 1996;33(3):239-52.
  48. Ziegert JC, Lewis JL. In-vivo mechanical properties of soft tissue covering bony prominences. *J Biomech Eng* 1978;100:194-201.

49. Mak AFT, Zheng YP. Biomechanical assessment of stump tissues using a force transducer in series with an ultrasound thickness gage (Abstract). Abstracts of the 8th World Congress of ISPO. Melbourne, Australia; 1995. p. 127.
50. Zheng YP, Mak AFT. Development of an ultrasound indentation system for biomechanical properties assessment of soft tissues in vivo. Proceedings of the 17th Annual International Conference of the IEEE Engineering in Medicine and Biology Society, Montreal, Canada; 1995. p. 1599-600.
51. Zheng YP, Mak AFT. Determination of the in-vivo incremental modulus of soft tissues using an ultrasound indentation system. 2nd Medical Engineering Week of the World, Taiwan; May 26-30, 1996.
52. Zheng YP, Mak AFT. An ultrasound indentation system for biomechanical properties assessment of soft tissues in vivo. *IEEE Trans Biomed Eng* 1996;43(9):912-8.
53. Zheng YP. Development of an ultrasound indentation system for biomechanical properties assessment of limb soft tissues in vivo (dissertation). Hong Kong Polytechnic University; 1997.
54. Hayes WC, Keer LM, Herrmann G, Mockros LF. A mathematical analysis for indentation tests of articular cartilage. *J Biomech* 1972;5:541-51.
55. Fung YC. Bio-viscoelastic solids. In: *Biomechanics: mechanical properties of living tissues*. New York: Springer-Verlag; 1981. p. 196-260.
56. Zhang M, Zheng YP, Mak AFT. Estimating the effective Young's modulus of soft tissues from indentation tests—nonlinear finite element analysis of effects of friction and large deformation. *Med Eng Phys* 1997;19:512-7.

Submitted for publication October 21, 1998. Accepted in revised form December 8, 1998.